

# Silicon carbide surface structure investigated by synchrotron radiation-based x-ray diffraction

H. Enriquez,<sup>a)</sup> M. D'angelo, V. Yu. Aristov,<sup>b)</sup> V. Derycke, and P. Soukiassian  
*Commissariat à l'Energie Atomique, Laboratoire Surfaces et Interfaces de Matériaux Avancés associé à l'Université de Paris-Sud/Orsay, DSM-DRECAM-SPCSI, Bâtiment 462, Saclay, 91191 Gif sur Yvette Cedex, France*

G. Renaud and A. Barbier  
*Commissariat à l'Energie Atomique, DSM-DRFMC-SP2M, 85 X, 38041 Grenoble Cedex, France*

S. Chiang  
*Department of Physics, University of California-Davis, Davis, California 95616-8677*

F. Semond  
*Centre National de la Recherche Scientifique, CRHEA, Sophia-Antipolis, 06650 Valbonne, France*

(Received 20 January 2003; accepted 17 April 2003; published 5 August 2003)

We use synchrotron radiation based x-ray diffraction at grazing incidence to study the atomic structure of Si-rich  $\beta$ -SiC(100)  $3 \times 2$  surface reconstruction. The latter includes three different Si atomic planes, in qualitative agreement with the theoretical two adlayers asymmetric dimer model. The measurements provide an accurate determination of the atomic bond, indicating asymmetric Si dimers in the first plane, and an alternating long and short Si dimers subsurface organization in the second atomic plane responsible for the lack of dimers buckling in the first plane, unlike corresponding silicon or germanium surfaces. © 2003 American Vacuum Society.

[DOI: 10.1116/1.1588650]

Silicon carbide (SiC) is a IV–IV wide band gap semiconductor that presents a strong interest for advanced electronic applications that cannot be fulfilled by conventional semiconductors, with average figures of merit scaling 2 or 3 orders of magnitude above those of all other semiconductors except diamond.<sup>1</sup> Beside its wide band gap, its high breakdown field, its high thermal conductivity and its high electron saturation velocity make it suitable for high-temperature, high-power, high voltage and high frequency applications. It is also resistant to radiation damage making which is especially useful for hostile environment.<sup>1</sup> Among the 170 existing polytypes, the  $\beta$ -SiC cubic phase crystallizes in the zinc-blend structure, with alternating silicon and carbon atomic planes in the (100) direction, so that one can expect some similarity to corresponding silicon or germanium surface structure.<sup>2</sup> But unlike Si or Ge, SiC is not a fully covalent semiconductor with polar (100) surfaces and stress playing a central role in surface ordering, since silicon and carbon atomic planes are, respectively, compressed by 20% and extended by 22%, as compared to the elemental Si and C semiconductors, respectively.<sup>1</sup> In the last decade, a control of the (100) surface has been achieved at the atomic scale, as evidenced by scanning tunneling microscope (STM) investigations.<sup>3–5</sup> Depending on the stoichiometry of the last few atomic planes, several reconstructions have been identified, involving a  $3 \times 2$  periodicity for the Si-rich surface, a  $c(4 \times 2)$  for the Si-terminated surface, a  $c(2 \times 2)$  for the C-terminated surface, and a C-rich  $1 \times 1$  for the graphitic phase. Reversible phase transitions have been observed be-

tween these different kinds of reconstruction simply by silicon deposition and/or thermal annealing.<sup>1</sup> The phase transition from the  $3 \times 2$  surface to the  $c(4 \times 2)$  one is of particular interest, since the silicon is removed in a selective way, leading to the formation of silicon atomic lines arrays, corresponding to successive  $5 \times 2$ ,  $7 \times 2$ ,  $9 \times 2$ ... reconstructions.<sup>5</sup>

The  $\beta$ -SiC(100) Si-terminated surface was earlier believed to have the same structure as the Si(100) surface, made of Si–Si dimers leading to a  $2 \times 1$  reconstruction.<sup>1</sup> But for surfaces prepared using high quality surface standards and excellent vacuum conditions, one could evidenced a  $c(4 \times 2)$  reconstruction instead of a  $2 \times 1$ , resulting from an alternative up and down dimers (AUDD) structure.<sup>4</sup> This specific  $c(4 \times 2)$  surface organization of symmetric dimers is believed to be primarily driven by the compressive surface stress applied on the silicon atomic planes. However, surface contamination and dimer vacancies can lead to a structural change from the  $c(4 \times 2)$  to a  $2 \times 1$  periodicity.<sup>4</sup> In contrast, the  $3 \times 2$  Si-rich surface has absolutely no equivalent on silicon surfaces.<sup>2</sup> First, this surface plays a specific role as a substrate for silicon atomic lines formation.<sup>5</sup> In addition, one striking feature is the very high sensitivity of this surface to oxygen adsorption, namely 3 orders of magnitude larger than silicon surfaces.<sup>6</sup> Although the atomic structure knowledge of this surface is crucial to understand its properties, it has not been solved yet. Indeed this structure was strongly debated during the last decade, giving rise to different competing models sketched in Fig. 1.<sup>3,7–12</sup>

The first observation of a  $3 \times 2$  surface reconstruction has been reported by Dayan nearly 2 decades ago on the basis of low energy electron diffraction (LEED) measurements.<sup>7</sup> To

<sup>a)</sup>Electronic mail: enriquez@cea.fr

<sup>b)</sup>On leave from: Russian Academy of Sciences, Chernogolovka, Moscow District, Russia.

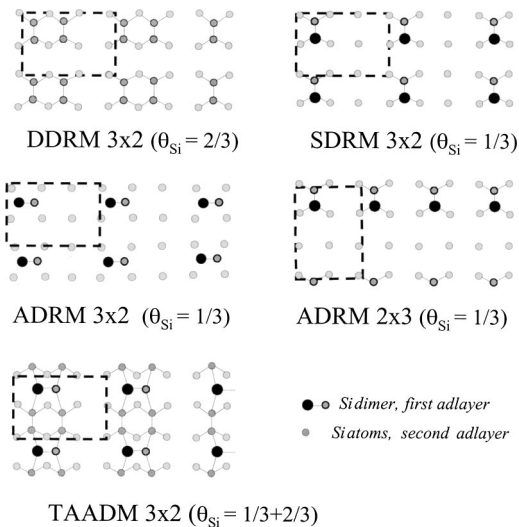


FIG. 1. Schematic top views of the  $\beta$ -SiC(001) $3\times 2$  surface reconstruction proposed models: (a) DDRM (Refs. 3, 6, and 8), (b) SDRM (Ref. 5), (c) ADRM  $2\times 3$  (Ref. 9), (d) ADRM  $3\times 2$  (Ref. 7) and TAADM (Ref. 10). The corresponding primitive  $3\times 2/2\times 3$  surface unit cell is indicated by a dashed line.

account for this periodicity, he has proposed a model involving two silicon atomic planes, with a  $2/3$  of monolayer (ML) surface plane on a full silicon atomic plane. In this model, the surface dimerisation leads to a  $\times 2$  periodicity along the Si–Si dimers, whereas one dimer over three is missing, leading to a  $\times 3$  periodicity in the perpendicular direction and to the  $2/3$  ML coverage. Subsequently, two dimers are included per unit cell, so that it is called the double dimer row model (DDRM), with dimers rows parallel to the dimer direction. But a few years later, Hara *et al.* has reported medium energy ion scattering (MEIS) experiments, deriving a  $1/3$  ML coverage for the last atomic plane instead of  $2/3$ .<sup>8</sup> On this basis, a single dimer row model (SDRM) has been proposed, with only one Si–Si dimer per unit cell. One should notice that the surface dimers are parallel to the  $\times 2$  direction in both DDRM and SDRM (Fig. 1). When the last atomic plane is removed, the underlying Si atomic plane can therefore form dimers, leading to a  $2\times 1$  or  $c(4\times 2)$  structure, in agreement with the experimental LEED observations.

Other nonstructural experiments such as valence band and core-level photoemission experiments or STM measurements are interpreted in the framework of the DDRM.<sup>9,10</sup> However, recent real-space atom-resolved STM measurements by Semond *et al.* tunneling into the unoccupied electronic states question both DDRM and SDRM.<sup>3</sup> Indeed, each spot observed in the occupied states splits in the unoccupied states into two spots of unequal intensities that can be assigned to individual atoms. Therefore, the Si atoms forming the dimers are resolved in the unoccupied states, and unambiguously indicate that the dimers are perpendicular to the dimer rows along the  $\times 2$  direction. On the ground of this STM observation, a sketch is proposed for the last surface plane, with asymmetric dimers perpendicular to the dimer rows and a total  $1/3$  ML coverage (Fig. 1).<sup>3</sup> However the STM technique is sensitive to the topmost atomic layer only, and cannot

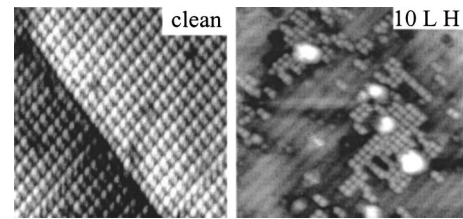


FIG. 2.  $\beta$ -SiC(100)- $3\times 2$  surface  $150\text{ \AA}\times 150\text{ \AA}$  STM topographs obtained by tunneling into empty states (tip bias  $-3\text{ V}$  with  $0.2\text{ nA}$  tunneling current), before and after 10 L atomic hydrogen exposure.

explain how these dimers, oriented along the  $\times 3$  direction, can be connected to the underlying Si atomic plane in order to agree with the experimental observation of a  $2\times 1/c(4\times 2)$  [and not a  $1\times 2/c(2\times 4)$ ] reconstruction for the Si-terminated surface.

At this point, some models are also derived from *ab initio* theoretical calculations. First, an asymmetric dimer row model (ADRM) has been proposed by Yan *et al.* and Pizzagalli *et al.* involving two silicon atomic planes, with a  $1/3$  ML coverage for the last plane.<sup>11</sup> In this model, the last atomic plane structure agrees with the sketch derived from the previous STM observations.<sup>3</sup> But this structure exhibits a  $2\times 3$  periodicity in strong contradiction with other experimental evidence (Fig. 1). Recently, another model was proposed by Lu *et al.*, the two adlayer asymmetric dimer row model (TAADM) involving three Si atomic planes instead of 2.<sup>12</sup> This TAADM model is the combination of the ADRM  $3\times 2$ <sup>3</sup> and DDRM,<sup>7,9</sup> where the first adlayer is identical to the ADRM  $3\times 2$  top  $1/3$  ML atomic plane and lies on a second adlayer similar to the DDRM top  $2/3$  ML atomic plane, instead of being directly connected to a Si-terminated surface.

The orientation of the topmost dimers has been questioned by the  $3\times 2$  to a  $3\times 1$  phase transition taking place upon atomic hydrogen exposure as reported by Hara *et al.* using LEED experiments.<sup>13</sup> Actually this transition has been assigned to Si–Si dimers breaking, which would imply that the dimers are parallel to the  $\times 2$  periodicity.<sup>13</sup> However, we have performed STM measurements in the unoccupied states before and after atomic hydrogen exposure with the surface kept at  $T=300\text{ }^\circ\text{C}$ . One can observe some reactive sites (Fig. 2), made of bright double spots of equal intensity, which correspond to reactive dimers becoming symmetric.<sup>14</sup> According to this STM observation, the reactive dimers are not broken. Furthermore, the general  $3\times 2$  surface ordering remains unchanged even if the surface is reactive.<sup>14</sup> Therefore, the  $3\times 1$  LEED structure reported by Hara *et al.* is not conclusive. One can rather interpret this observation by a defect-induced lost of  $\times 2$  long-range periodicity. Actually, even on clean surfaces, one can observe the so-called “dimer-pair defect” and the correlated one-half unit cell parameter shift along the dimer row.<sup>3</sup> This kind of defect is leading to long antiphase boundaries and it is responsible for the long-range periodicity weakening along the  $\times 2$  direction. Such an effect existing on the clean surface may indeed be enhanced by atomic hydrogen interaction. Notice also that such a  $3\times 1$

LEED pattern has been observed to result from oxygen contamination.<sup>7</sup>

In order to discriminate between these various models, some valence-band spectroscopy photoemission experiments<sup>10</sup> have been revisited by Lu *et al.* in order to compare experimental data to theoretical calculations.<sup>12</sup> The available data can find some agreement with the surface bands calculated for the TAADM only, whereas both DDRM and SDRM are ruled out. However, such a comparison cannot be conclusive since there are very few available experimental data, and especially no data along the dispersing  $J-M$  and  $M-J'$  directions. Also some reflectance anisotropy spectroscopy measurements have been performed<sup>15</sup> and experimental data compared to theoretical calculations, but in that case, it is really difficult to discriminate between TAADM and DDRM which both exhibits two similar broad spectral features.<sup>16</sup>

A structural tool is therefore required to discriminate between the models. For this purpose, we turn to grazing incidence x-ray diffraction (GIXRD), which has been especially successful in solving accurately complex surface structures.<sup>17</sup> The GIXRD experiments using synchrotron radiation are performed on the CRG-IF (BM32) beam line (ESRF, Grenoble) at a  $3 \times 10^{-11}$  Torr pressure, keeping a very high surface quality during the all measurements. Because of the lack of high-quality cubic SiC single crystals, such an experiment has been done on a single crystal thin film (1  $\mu\text{m}$ ). This latter is grown by chemical vapor deposition on a carbonized Si(100) wafer with a buffer layer at the SiC/Si interface having rather large stacking fault defect densities, making surface measurements especially challenging. In order to eliminate the contribution coming from the stacking faults, we use a low photon energy at 12 keV, below the critical angle value. As compared to a standard semiconductor study, the probed reciprocal space area is therefore reduced. In addition, a specific sample mounting is needed for homogeneous high temperature annealings through direct current heating, reducing further the probed area. High quality  $\beta$ -SiC(001) $3 \times 2$  single domain surfaces are checked by reflection high energy electron diffraction and GIXRD. The basis vectors ( $a_s, b_s, c_s$ ) of the surface reconstruction unit cell are related to the bulk ones by  $\mathbf{a}_s = [1 \bar{1} 0]_{\text{bulk}}$ ,  $\mathbf{b}_s = [110]_{\text{bulk}}$ ,  $\mathbf{c}_s = [001]_{\text{bulk}}$ , with  $a_s = b_s = 3.088 \text{ \AA}$  and  $c_s = 4.367 \text{ \AA}$ . The reciprocal space is described by its reduced coordinates ( $h, k, l$ ),  $l$  being perpendicular to the surface. Two complete sets of data (measured from two distinct  $3 \times 2$  surfaces) are in excellent agreement. For each set, we measure 78 inequivalent in-plane and 276 out-of plane reflections, along eight inequivalent rods, and 168 reflections along five inequivalent crystal truncation rods (CTRs).<sup>17</sup> Details about high quality  $3 \times 2$  surface preparation and GIXRD can be found elsewhere.<sup>1,3,17</sup> For the analysis, we do not take into account the diffracted intensities along the  $\times 2$  direction which are too weak likely resulting from Si dimer pairs formation (defect B) as identified by atom resolved STM.<sup>3</sup>

From the in-plane diffracted intensities, measured at  $l = 0.05$ , we derive the experimental Patterson function shown

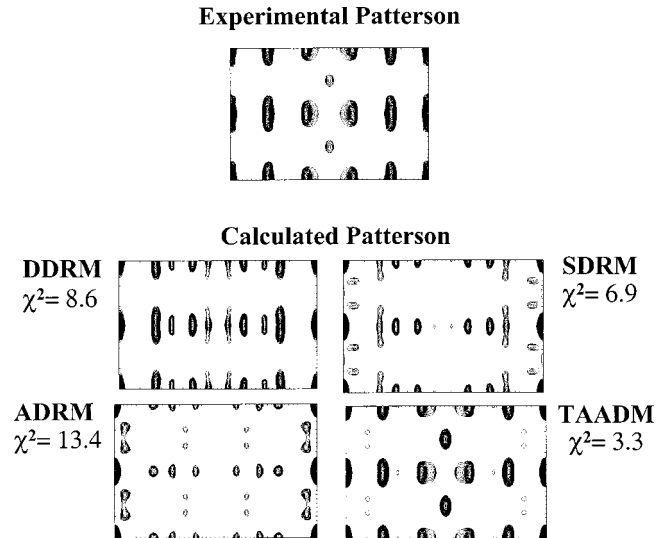


FIG. 3. Experimental and calculated Patterson function maps for the different existing models. The experimental Patterson function is derived from the in-plane diffracted intensity of the  $\beta$ -SiC(001) $3 \times 2$  surface measured at  $l = 0.05$ . The calculated Patterson functions are derived from the fit of the first adlayer atomic positions assuming a  $p2mm$  symmetry. The corresponding  $\chi^2$  agreement factors are also displayed for each model.

in Fig. 3 and therefore, we can determine the in-plane interatomic vectors in the unit cell.<sup>17</sup> The experimental Patterson function exhibits a  $p2mm$  symmetry that is consistent with either a  $p2mm$  (two perpendicular mirrors),  $p1m$  (one mirror), or  $pm1$  symmetry of the unit cell. First, we compare the experimental diffracted intensities with the calculated ones for each model, in the framework of a  $p2mm$  symmetry. Therefore, we fit the atomic positions of the first adlayer for each model. The different models can be evaluated through the least-square residual agreement factor  $\chi^2$  that takes into account a 10% experimental error bar. As displayed in Fig. 3, all models yield  $\chi^2$  values much larger than the satisfactory value of 1 with 13.4 for the ADRM, 8.6 for the DDRM, 6.9 for the SDRM, the TAADM being the closest at  $\chi^2 = 3.3$ . For comparison, the corresponding calculated Patterson functions are shown in Fig. 3.

Therefore, we choose the TAADM as a starting point, and we fit the in-plane diffracted intensities by relaxing also the in-plane atomic positions of the underlying atomic planes. However, within the  $p2mm$  symmetry, one cannot achieve a  $\chi^2$  better than 2.5. Therefore, we reduce the symmetry conditions and perform the fit on the basis of a  $p1m$  symmetry. The top dimer is therefore allowed to be asymmetric while the underlying dimers may have different lengths. Using this fitting procedure, the least mean square residual minimization leads to a  $\chi^2 = 1.4$  value for the reconstruction in-plane intensities. Thus, we conclude on the  $p1m$  symmetry, and we apply the fitting procedure to the whole data set, including both in-plane and out-of-plane reconstruction rods intensities, leading to a very satisfactory  $\chi^2 = 1.2$  factor. This fitting agreement is illustrated in Fig. 4 by the comparison between the experimental and the calculated Patterson functions. The diffracted intensities along the surface rods give some in-

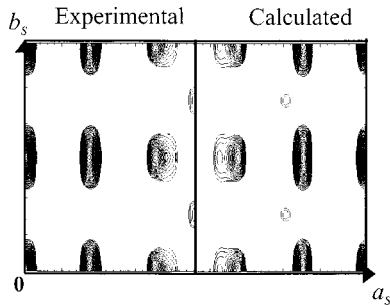


FIG. 4. Experimental (right) and calculated (left) half Patterson contour plots for the ALSD model of the  $\beta$ -SiC(001) $3\times 2$  surface reconstruction, represented over the whole  $3\times 2$  unit cell. 50 contour levels are used between the 0.14 and 1 minimal and maximal values. The fitting procedure is performed for the in- and out-of-plane reconstruction rods data in the framework of a  $\rho 1m$  symmetry.

sights about the out-of-plane atomic positions. Four different representative profiles are shown in Fig. 5, along the  $(5-2l)$ ,  $(50l)$ ,  $(10l)$  and  $(80l)$  surface reconstruction rods. The fitting curve average modulation period is found between 2.5 and 2.8 in the reciprocal lattice coordinates, which corresponds to a 2.3 Å direct space thickness, indicating that the reconstruction involves more than two silicon atomic layers.

The previous fitting procedure allows determining the in-plane and out-of-plane coordinates of the 12 atoms involved

per reconstruction unit cell. First, we notice that the silicon atomic planes are distant by  $a_0/3$ ,  $a_0$  being the unit lattice parameter, instead of  $a_0/4$ , the bulk interlayer distance, evidencing the open character of the surface. The dimers of the first adlayer are found to be asymmetric, in agreement with the STM measurements,<sup>3</sup> but the results indicate a 0.1 Å height difference, much less than the calculated height at 0.5 Å in the TAADM. The most striking feature is that the underlying dimers of the second adlayer have different lengths, namely a long one at 2.41 Å and a short one at 2.26 Å, in contrast with the TAADM where both dimers were calculated to have the same length at 2.37 Å, somewhat closer from the long dimer. The alternating long ( $D_L$ ) and short ( $D_S$ ) dimers are bonded on both sides, respectively, to the up ( $A_U$ ) and down ( $A_D$ ) atoms of the top asymmetric dimers.

The CTR could be fitted with a  $\chi^2=2.5$  indicating a rather flat surface with a negligible roughness ( $\beta=0.08$ ). Two representative profiles are shown in Fig. 5 for the  $(60l)$  and the  $(30l)$  CTR. From the  $(300)$  anti-Bragg reflection, one can deduce a 300 Å average terrace length, in agreement with STM measurements.<sup>3</sup> According to the CTR fit, the surface reconstruction is registered to bulk with slight deviations ( $\Delta x=0.03$  Å,  $\Delta z=0.03$  Å) of the deeper third silicon atomic plane atoms from bulk positions.

The alternative long and short dimers (ALSD) model derived from our grazing incidence x-ray diffraction data

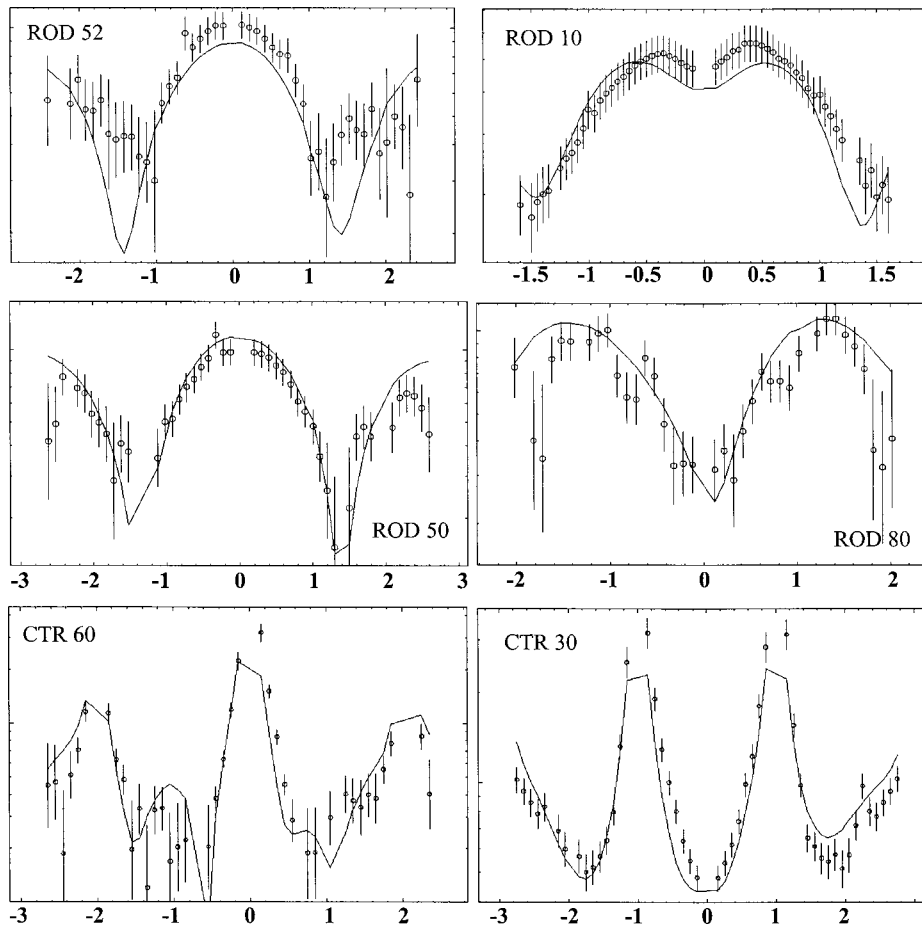


FIG. 5.  $(5-2l)$ ,  $(10l)$ ,  $(50l)$ , and  $(80l)$  surface reconstruction rods and  $(60l)$  and  $(30l)$  CTR profiles with the error bars and corresponding fits. The logarithm of the absolute value of the structure factor is represented as a function of the out-of-plane reciprocal lattice coordinate  $l$ .



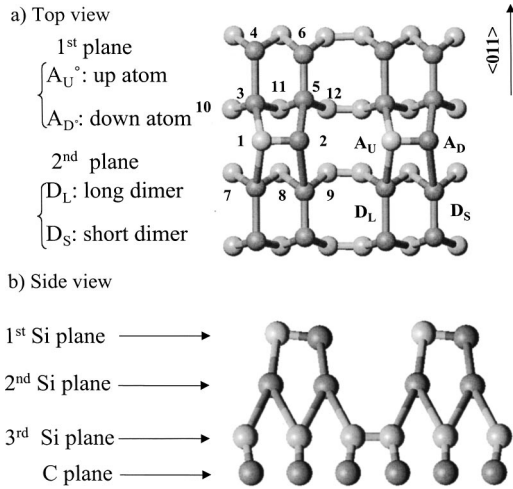


FIG. 6. (a) Top and (b) side views of the  $\beta$ -SiC(001) $3 \times 2$  surface reconstruction showing the three Si atomic planes with the top  $A_U$ - $A_D$  asymmetric dimers (first plane) and the ALSD dimers having alternating long  $D_L$  and short  $D_S$  lengths in the second plane.

analysis is sketched in Fig. 6. The structure is in agreement with the theoretical TAADM for the surface morphology, involving three Si atomic planes with respective  $1/3$  ML and  $2/3$  ML for the first and second adlayers that are lying on a third full atomic silicon plane. However, the second silicon adlayer presents a long-range organization with alternating long and short dimers (ALSD) that was not predicted in the *ab initio* calculations.<sup>12</sup> Surface stress minimization is already known to be responsible for the Si-terminated AUDD surface structure.<sup>4</sup> In the  $3 \times 2$  structure, this silicon atomic plane becomes the third deeper one, and in this configuration, is lying very close from the bulk atomic positions. One can therefore imagine that the stress has been “transferred” to the next silicon plane. In this view, the second adlayer is expected to minimize the surface stress and to encounter a kind of AUDD reconstruction. Actually, the stress minimization is occurring in a slightly different way, probably because a  $1/3$  ML Si plane is lying above, leading to the ALSD structure to develop instead of an AUDD one. Furthermore, this long-range organization of the second adlayer can explain why all the dimers of the first adlayer are tilted in the same direction. The ALSD model of the  $\beta$ -SiC(100)  $3 \times 2$  surface reconstruction determined here is in excellent agreement with recent photoelectron diffraction experiments.<sup>18</sup>

In conclusion, we have determined the atomic structure of the Si-rich  $\beta$ -SiC(100)  $3 \times 2$  surface reconstruction using GIXRD. The results indicate that the DDRM, SDRM, and ADRM  $2 \times 3$  models are not suitable for the  $3 \times 2$  reconstruction, but in qualitative agreement with the TAADM model. However, we evidenced a subsurface layer having alternating long (2.41 Å) and short (2.26 Å) dimers. This

subsurface organization allows strain minimization and influences the topmost atomic plane, leading to an array of asymmetric dimers all tilted in the same direction with no buckling, in strong contrast to the situation occurring for asymmetric dimer on Si(001) and Ge(001) surfaces.

## ACKNOWLEDGMENTS

The authors are grateful to Marion Noblet and to the ESRF (Grenoble) staff for expert technical assistance, to Lea di Cioccio, Thierry Billon, and Catherine Pudda (CEA-LETI, Grenoble) for providing high quality  $\beta$ -SiC(100) thin films, and to E. Vlieg for the use of his ROD program. One of us (V. Yu. A.) thanks the RFBR for Grant No. 02-02-16811.

<sup>1</sup>Silicon Carbide, *A Review of Fundamental Questions and Applications to Current Device Technology*, edited by W. J. Choyke, H. M. Matsunami, and G. Pensl (Akademie Verlag, Berlin, 1998), Vols. I & II; V. M. Bermudez, *ibid.*, p. 447; P. Soukiassian, *Mater. Sci. Eng.*, B **61**, 506 (1999), and references therein.

<sup>2</sup>C. B. Duke, *Chem. Rev. (Washington, D.C.)* **96**, 1237 (1996); J. A. Kubby and J. J. Boland, *Surf. Sci. Rep.* **26**, 63 (1996).

<sup>3</sup>F. Semond, P. Soukiassian, A. Mayne, G. Dujardin, L. Douillard, and C. Jaussaud, *Phys. Rev. Lett.* **77**, 2013 (1996).

<sup>4</sup>P. Soukiassian, F. Semond, L. Douillard, A. Mayne, G. Dujardin, L. Pizzagalli, and C. Joachim, *Phys. Rev. Lett.* **78**, 907 (1997).

<sup>5</sup>P. Soukiassian, F. Semond, A. Mayne, and G. Dujardin, *Phys. Rev. Lett.* **79**, 2498 (1997); L. Douillard, V. Yu. Aristov, F. Semond, and P. Soukiassian, *Surf. Sci. Lett.* **401**, L395 (1998); V. Yu. Aristov, L. Douillard, and P. Soukiassian, *ibid.* **440**, L825 (1999).

<sup>6</sup>F. Semond, L. Douillard, P. Soukiassian, D. Dunham, F. Amy, and S. Rivillon, *Appl. Phys. Lett.* **68**, 2144 (1996); F. Amy, H. Enriquez, P. Soukiassian, P. F. Storino, Y. J. Chabal, A. J. Mayne, G. Dujardin, Y. K. Hwu, and C. Brylinski, *Phys. Rev. Lett.* **86**, 4342 (2001).

<sup>7</sup>M. Dayan, *J. Vac. Sci. Technol. A* **3**, 361 (1985); **4**, 38 (1986).

<sup>8</sup>S. Hara, W. F. J. Slijkerman, J. F. van der Veen, I. Ohdomari, S. Misawa, E. Sakuma, and S. Yoshida, *Surf. Sci. Lett.* **231**, L196 (1990).

<sup>9</sup>S. Hara, S. Misawa, S. Yoshida, and Y. Aoyagi, *Phys. Rev. B* **50**, 4548 (1994).

<sup>10</sup>H. W. Yeom, Y. C. Chao, S. Terada, S. Hara, S. Yoshida, and R. I. G. Uhrberg, *Phys. Rev. B* **56**, R15525 (1997); H. W. Yeom, Y. C. Chao, I. Matsuda, S. Hara, S. Yoshida, and R. I. G. Uhrberg, *ibid.* **58**, 10540 (1998); M. Lübke, K. Lindner, S. Sloboshanin, S. Tautz, J. Schafer, and D. R. T. Zahn, *J. Vac. Sci. Technol. A* **16**, 3471 (1998).

<sup>11</sup>H. Yan, A. P. Smith, and H. Jónsson, *Surf. Sci.* **330**, 265 (1995); L. Pizzagalli, A. Catellani, G. Galli, F. Gygi, and A. Baratoff, *Phys. Rev. B* **60**, R5129 (1999).

<sup>12</sup>W. Lu, P. Krüger, and J. Pollmann, *Phys. Rev. B* **60**, 2495 (1999).

<sup>13</sup>S. Hara, S. Misawa, S. Yoshida, and Y. Aoyagi, *Phys. Rev. B* **50**, 4548 (1994); H. W. Yeom, I. Matsuda, Y. C. Chao, S. Hara, S. Yoshida, K. Kajimura, and R. I. G. Uhrberg, *ibid.* **61**, R2417 (2000).

<sup>14</sup>V. Derycke, P. Soukiassian, F. Amy, Y. Chabal, M. D’angelo, H. Enriquez, and M. Silly, *Nature Mater.* **2**, 253 (2003).

<sup>15</sup>U. Rossow, K. Lindner, M. Lübke, D. E. Aspnes, and D. R. T. Zhan, *J. Vac. Sci. Technol. B* **16**, 2355 (1998).

<sup>16</sup>W. Lu, W. G. Schmidt, E. L. Briggs, and J. Bernholc, *Phys. Rev. Lett.* **85**, 4381 (2000).

<sup>17</sup>R. Feidenhans’l, *Surf. Sci. Rep.* **10**, 105 (1989); I. K. Robinson and D. J. Tweet, *Rep. Prog. Phys.* **55**, 599 (1992); G. Renaud, *Surf. Sci. Rep.* **32**, 1 (1998).

<sup>18</sup>A. Tejada, E. Garcia-Michel, D. Dunham, P. Soukiassian, J. Drenlinger, E. Rotenberg, Z. Hurych, and B. Tonner, recent photoelectron diffraction investigation using synchrotron radiation at the Advanced Light Source, Berkeley.